Eur. Phys. J. D **24**, 269–272 (2003)
DOI: 10.1140/epjd/e2003-00171-0

THE EUROPEAN PHYSICAL JOURNAL D

Silicon-riched-oxide cluster assembled nanostructures formed by low energy cluster beam deposition

M. Han[1,a], J.F. Zhou[1], F.Q. Song[2], C.R. Yin[2], M.D. Liu[1], J.G. Wan[2], and G.H. Wang[2]

[1] National Laboratory of Solid State Microstructures, Department of Materials Science and Engineering, Nanjing University, Nanjing 210093, P.R. China
[2] National Laboratory of Solid State Microstructures, Department of Physics, Nanjing University, Nanjing 210093, P.R. China

Received 10 September 2002
Published online 3 July 2003 –

Abstract. Free beam of silicon oxide nanoclusters is produced by a gas aggregation source from SiO precursor. Due to the disproportionation reaction during the condensation of SiO vapor the generated clusters are Si-riched. The clusters are collimated to be a fine beam and deposited on the substrate at room temperature. The microstructures of the cluster-based nanofilm are characterized by TEM. It is shown that with appropriate impacting parameters, Si-riched oxide nanofilms assembled from uniformly distributed isolated clusters can be obtained. And the clusters can self-organize into partially densely ordered packing within local domains. XPS spectra are taken to analyze the chemical components of the nanofilms. Photoluminescence from the Si-riched oxide nanofilms has also been observed.

PACS. 36.40.Sx Diffusion and dynamics of clusters – 61.46.+w Nanoscale materials: clusters, nanoparticles, nanotubes, and nanocrystals – 81.07.-b Nanoscale materials and structures: fabrication and characterization

1 Introduction

The atomic clusters deposited from gas phase under UHV-compatible condition have been recently used as building blocks for the controlled synthesis of nanostructure, whose structure is well defined on the nanoscale and allows unprecedented novel optical, electronic, magnetic properties. In addition, a wide variety of characterization techniques can be used to monitor all the stages of cluster assembling so as to freely control the process parameters such as the cluster mass and energy distribution, the cluster landing energy as well as the cluster diffusion and interaction [1]. Moreover, cluster-assembled nanostructured materials show enormous potential applications, and the technique developed for depositing gas phase clusters will be used in industrial process within a decade [2].

On the other hand, the fundamental mechanism underlying cluster assembling, especially the self-organizing of nanoclusters into regular arrays on large area of substrate surface is still poorly understood [3]. Surface kinetics, which depends critically on the phenomena concerning cluster landing, diffusion and interaction on the surface is very complex [2,4] and needs to be further investigated.

Recently, the silicon-riched-oxide (SRO) nanostructures have been observed interesting optical and electrical properties such as the visible photoluminescence (PL) and electroluminescence (EL), as well as cold electron emission, tunneling, demonstrating its potential application of silicon-based nanodevice and flat panel field emission displays [5,6]. For such purpose, high density regular array of SRO nanoclusters uniformly distributed on two dimension is the fundamental requirement. Gas phase cluster deposition is the viable route compatible to the industrial process, however, approaches from gas phase deposition of SRO nanoclusters usually generate undesired aggregated structures [7]. The deposited clusters stick irreversibly and form fractal like aggregates [8]. The spatial distribution of the clusters is irregular and nonuniform.

In this paper, we report the successful generation of uniform arrays of isolated silicon-riched-oxide nanoclusters by low energy cluster beam deposition (LECBD). The SRO nanoclusters are composed of small embedded silicon clusters and exhibit photoluminescence properties. The morphology of the SRO cluster assembled nanostructures and the correlation of the clusters are analyzed.

2 Experimental

To prepare the silicon oxide cluster-based nanofilm, we use low energy cluster beam deposition (LECBD) method [9]. Free beam of nanoclusters is produced by a Sattler type

[a] e-mail: sjhanmin@nju.edu.cn

gas aggregation source from SiO precursor. The main feature of the differentially pumped cluster beam formation and deposition system has been fully described elsewhere [10]. Briefly, the source is operated at constant helium flow. The pressure in the source chamber is maintained at ∼10 torr. The chamber wall is cooled to liquid nitrogen temperature. SiO powder of 99.99% purity is evaporated from a BN oven heated to 1300 K. The oven is sufficiently screened by heat reflectors to avoid thermal radiation to the condensation space. Hot vapor emerges into the He atmosphere through an orifice of 1.0 mm diameter. A large number of collisions among the vapor and cold buffer gas cause efficient cluster nucleation. During the quick condensation of SiO vapor, a portion of the SiO molecular is decomposed of Si and SiO_2 due to the following disproportionation reaction:

$$2SiO \rightarrow SiO_2 + Si.$$

As a result, the generated clusters are Si-riched. The clusters leave the source chamber through an expansion nozzle and pass the two differential pumping stages separated with a skimmer and a collimator of 2 mm diameter each. A fine beam of clusters is formed and deposited on the substrate, situated at a distance of 400 mm from the expansion nozzle. The substrate is kept at room temperature. The deposition chamber is maintained in the upper 10^{-7} torr range and the deposition rate is ∼2 Å/s as measured by a quartz microbalance system. The spot of the deposition has a typical diameter of 10 mm, indicating that the divergence angle of the cluster beam is as small as 2°. The use of highly collimated cluster beam allows a very precisely control of the impacting momentum of the clusters through directed cluster beam deposition. Therefore the diffusion of the clusters on the surface and the cluster-cluster sintering behavior, which are two important factors to the morphology of the developed cluster assembled nanofilms, can be finely controlled. In the present work, the normal incidence condition is examined. Copper grids covered with amorphous carbon film are used as substrates for transmission electron microscopy (TEM) observation. A JEM-200CX electron microscope operated at 200 keV is used. The cluster assembled nanofilm is also characterized by X-ray photoelectron spectroscopy (XPS) as well as photoluminescence measurements. Fused silica is used as substrate for such measurements.

3 Results and discussion

Typical cluster-based nanostructures formed by cluster beam deposition, as revealed by TEM, is illustrated in Figure 1a. The deposition rate and the deposition time is controlled so that a monolayer of clusters is formed on the surface. The clusters show a fairly uniform distribution on the long range scale, having the character of a statistical deposition from the gas phase. On the short range scale, the clusters are densely located on two dimension, keeping isolated from each other. No coagulations can be observed.

We also deposit silicon oxide clusters formed by inert gas condensation process in the static He atmosphere.

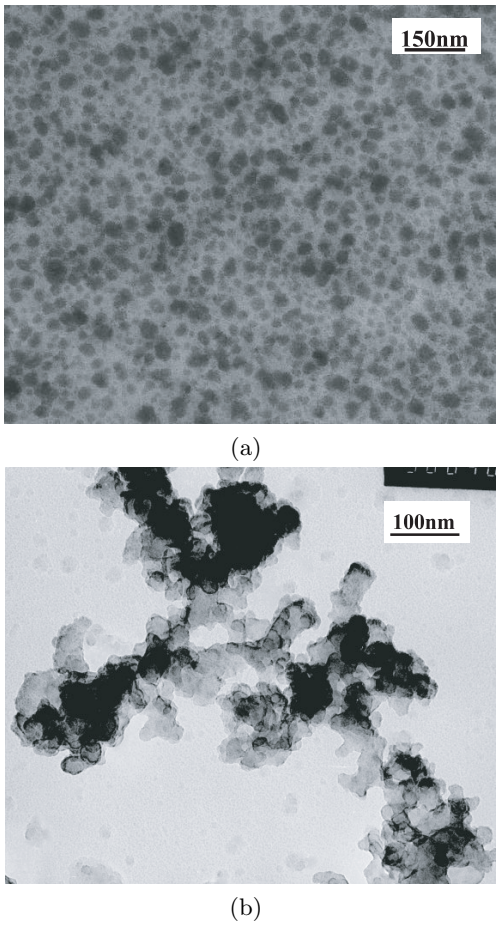

Fig. 1. (a) TEM micrograph of the silicon-riched-oxide nanostructured film assembled from low energy cluster beam deposition. (b) TEM micrograph of silicon oxide cluster aggregates with fractal structures.

The substrate is hung 15 cm away from the cluster source. Since the source is sufficiently heat screened, the substrate suffers no direct heat radiation from the source. The temperature of the substrate can thus be expected to be lower than the room temperature due to the cooling by the cold inert gas, which is cooled by the liquid nitrogen. In this case, coagulation structures on large scale are formed with silicon oxide nanoclusters (shown in Fig. 1b).

The coagulations are usually formed by irreversibly sticking together of clusters without coalescence. In the static inert gas atmosphere, the clusters arrive the substrate through diffusion. The mean free path of the clusters is very short. The residence time of the clusters in the inter gas atmosphere is much higher than that of the clusters in the beam source, which is differentially pumped and instantaneously extracts the clusters to high vacuum. As a result, the cluster density of the local region between the source and substrate is high. There are a large number of collisions between the clusters in the diffusion path before they deposit. The clusters move randomly on the gas phase as well as on the surface, sticking irreversibly when they collide, giving rise to the three-dimensional fractal aggregation on large scale. In the case of cluster beam

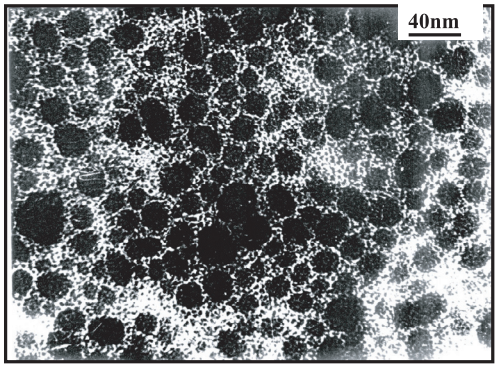

Fig. 2. TEM micrograph which shows partially ordered close packing morphology appears locally in mediate lengths.

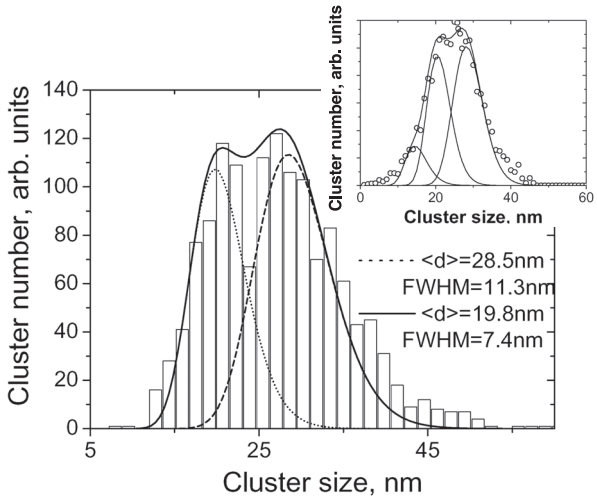

Fig. 3. Cluster size distribution function for the silicon-riched-oxide nanostructured film assembled from low energy cluster beam deposition. The bar chart gives the measurement results from TEM micrograph. The size distribution is fitted by two log-normal functions, shown by the dotted line and the dashed line respectively. The solid line gives the sum of the two components. The inset graph shows the simulation result, which can also be fitted by several log-normal functions.

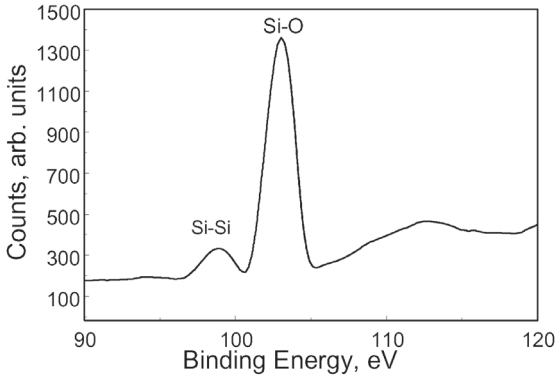

Fig. 4. Si 2*p* XPS spectrum of the silicon-riched oxide cluster assembly.

deposition, however, the clusters are rapidly brought to the exit nozzle by the inert gas flow and deposited on the substrate under high vacuum condition. The draft speed is much higher than the diffusion speed so that the residence time for the clusters in the inert gas atmosphere is much shorter. Therefore, the clusters undergo few cluster-cluster collisions on gas phase. The diffusion range on the substrate surface is also small for the normal incident clusters in highly collimated beam. As a result, coagulation can be avoided and the long-range morphology of the film is very uniform.

Translationally ordered close-packing morphology can be observed locally (on sub-micron scale), as shown in Figure 2, although the silicon oxide nanostructure formed by cluster beam deposition shows a uniform random distribution on the long-range scale. The partially developed ordered pattern can be extended to a range of 3 nearest neighbor spacing or more on average.

In the low energy cluster beam deposition, the kinetic energy for clusters is several ten meV/atom or below at a rough estimate, implying that the clusters can land on the substrate surface without breaking. For the normal incident deposition, the cluster velocity tangential to the substrate surface is only a few percent of the incident velocity, as can be estimated from the divergence of the collimated beam. Therefore after landing on the surface, the clusters have only kinetic energies of the order of meV, which are not high enough to serve for the surface diffusion energy. This implies that the clusters can migrate only in a limited length when they land on the substrate surface. During the migration, smaller clusters tend to coalesce to form new larger ones when they collide while lager clusters get to be saturated [11] — the coalescence process ceases. The saturation feature keeps the clusters isolated each other rather than sticking together to form a fractal aggregation. With moderate deposition rate, a balance may be reached among the arrival rate of clusters to the local domain, the limited diffusion range and the coalescence mechanism. In this case, the clusters confined within a local domain may organize into partial order.

The size distribution of the clusters in the deposited film is calculated from the TEM micrograph and shown in Figure 3. The mean size of the cluster assembly is about 26 nm. The size distribution curve has several peaks and shoulders. There is enough sampling number to obtain the size distribution so as to rule out the statistical fluctuation origin of the peak splitting. The size distribution curve can be decomposed to at least two log-normal distribution function, as shown in Figure 3. Such features may arise from the limited coalescence and surface diffusion mechanism we discussed above. A computer simulation based upon the same assumptions for the mechanism of low energy cluster beam deposition gives similar multi-peak feature on the size distribution function (see the inset graph of Fig. 3). The detail of the calculation can be found in reference [11].

Figure 4 presents the Si 2*p* XPS spectrum measured from the as-deposited silicon oxide cluster-based film. Besides the peak in the binding energy range of ∼103.5 eV, which is characteristic for oxidized silicon, the spectrum

also shows the presence of a peak at ∼99 eV assigned to Si–Si bonds of element silicon, confirming the Si-riched-oxide composition of the generated clusters.

Photoluminescence can also be observed from our Si-riched-oxide nanofilms assembled from cluster beam deposition. The PL band may be attributed to quantum confinement effect of small Si clusters embedded in the SiO_x nanoparticles. The detail of the investigation is presented elsewhere [12].

4 Conclusion

Si-riched-oxide cluster-assembled nanostructured films are synthesized by low energy cluster beam deposition from SiO precursor. With appropriate impact parameters, such nanofilms can be obtained by densely and uniformly distributed isolated clusters with partially ordered structure within local domains. The Si-riched-oxide composition of the generated clusters is confirmed by XPS measurement. The Si-riched-oxide nanofilm exhibits photoluminescence, which may be attributed to the presence of the individual small Si clusters inside the SiO_x nanoparticles.

This work was supported by the National Natural Science Foundation of China (Grant No. 10274031) and the Analysis and Measurement Foundation of Nanjing University.

References

1. E. Barborini, F. Siviero, S. Vinati, C. Lenardi, P. Piseri, P. Milani, Rev. Sci. Instrum. **73**, 206 (2002)
2. C. Binns, Surf. Sci. Rep. **44**, 1 (2001)
3. P. Jensen, Rev. Mod. Phys. **71**, 1695 (1999)
4. M. Han, Y. Gong, J. Ma, F. Liu, G. Wang, Surf. Rev. Lett. **3**, 91 (1996)
5. H. Rinnert, M. Vergnat, G. Marchal, Mat. Sci. Eng. B **69-70**, 484 (2000)
6. C. Busseret, A. Souifi, T. Baron, S. Monfray, N. Buffet, E. Gautier, M.N. Semeria, Mat. Sci. Eng. C **19**, 237 (2000)
7. H. Hofmeister, P. Ködderitzsch, J. Dutta, J. Non-Cryst. Solids **232-234**, 182 (1998)
8. C. Bréchignac, Ph. Cahuzac, F. Carlier, C. Colliex, J. Leroux, A. Masson, B. Yoon, U. Landman, Phys. Rev. Lett. **88**, 196103 (2002)
9. G. Fuchs, M. Treilleux, F. Santos Aires, B. Cabaud, P. Melonon, A. Hoareau, Phys. Rev. B **40**, 6128 (1989); P. Melinon, V. Pallard, V. Dupuis, A. Perez, P. Jensen, A. Hoareau, J.P. Perez, J. Tuaillon, M. Broyer, J.L. Vialle, M. Pellarin, B. Baguenard, J. Lerme, Int. J. Mod. Phys. B **9**, 339 (1995)
10. M. Han, G.H. Wang, *Proceedings of International Workshop on Cluster Science and Atomic Engineering*, Nan Deihe, China, Tianjing Univ. Press, China, 1997, p. 188
11. M. Han, Z.Y. Wang, P.P. Chen, S.W. Yu, G.H. Wang, Nucl. Instr. Meth. Phys. Res. B **135**, 564 (1998)
12. J.G. Wan, M. Han, J.F. Zhou, G.H. Wang, Phys. Lett. A **280**, 357 (2001)